



Shear strength criteria for rock, rock joints, rockfill and rock masses: Problems and some solutions

Nick Barton

Nick Barton & Associates, Oslo, Norway

ARTICLE INFO

Article history:

Received 6 July 2012

Received in revised form 27 July 2012

Accepted 2 October 2012

Keywords:

Rock masses
Critical state
Rock joints
Shear strength
Non-linear friction
Cohesion
Dilation
Scale effects
Numerical modelling
Stress transforms

ABSTRACT

Although many intact rock types can be very strong, a critical confining pressure can eventually be reached in triaxial testing, such that the Mohr shear strength envelope becomes horizontal. This critical state has recently been better defined, and correct curvature or correct deviation from linear Mohr–Coulomb (M-C) has finally been found. Standard shear testing procedures for rock joints, using multiple testing of the same sample, in case of insufficient samples, can be shown to exaggerate apparent cohesion. Even rough joints do not have any cohesion, but instead have very high friction angles at low stress, due to strong dilation. Rock masses, implying problems of large-scale interaction with engineering structures, may have both cohesive and frictional strength components. However, it is not correct to add these, following linear M-C or nonlinear Hoek–Brown (H-B) standard routines. Cohesion is broken at small strain, while friction is mobilized at larger strain and remains to the end of the shear deformation. The criterion ‘ c then $\sigma_n \tan \varphi$ ’ should replace ‘ c plus $\sigma_n \tan \varphi$ ’ for improved fit to reality. Transformation of principal stresses to a shear plane seems to ignore mobilized dilation, and caused great experimental difficulties until understood. There seems to be plenty of room for continued research, so that errors of judgement of the last 50 years can be corrected.

© 2013 Institute of Rock and Soil Mechanics, Chinese Academy of Sciences. Production and hosting by Elsevier B.V. All rights reserved.

1. Introduction

Non-linear shear strength envelopes for intact rock and for (non-planar) rock joints are the reality, but traditional shear test interpretation and numerical modelling in rock mechanics has ignored this for a long time. The non-linear Hoek–Brown (H-B) criterion for intact rock was eventually adopted, and many have also used the non-linear shear strength criterion for rock joints, using the Barton and Choubey (1977) wall-roughness and wall-strength parameters JRC (joint roughness coefficient) and JCS (joint compressive strength).

Non-linearity is also the rule for the peak shear strength of rockfill. It is therefore somewhat remarkable why so many are still wedded to the ‘ $c + \sigma_n \tan \varphi$ ’ linear strength envelope format.

E-mail address: nickrbarton@hotmail.com

Peer review under responsibility of Institute of Rock and Soil Mechanics, Chinese Academy of Sciences.



1674-7755 © 2013 Institute of Rock and Soil Mechanics, Chinese Academy of Sciences. Production and hosting by Elsevier B.V. All rights reserved.
<http://dx.doi.org/10.1016/j.jrmge.2013.05.008>

Simplicity is hardly a substitute for reality. Fig. 1 illustrates a series of simple strength criteria that predate H-B, and that are distinctly different from Mohr–Coulomb (M-C), due to their non-linearity.

The actual shear strength of rock masses, meaning the prior failure of the intact bridges and then shear on the fractures and joints at larger strains, is shown in Fig. 1 (units of σ_1 and σ_2 are in MPa).

2. Intact rock

The three-component based empirical equations (using roughness, wall strength and friction) shown in Fig. 1 were mostly derived in Barton (1976). The similarity of shear strength for rock joints and rockfill was demonstrated later in Barton and Kjærnsli (1981).

At the time of this mid-seventies research by the writer, it was recognized that the shear strength envelopes for intact rock, when tested over a wide range of confining stress, would have marked curvature, and eventually reach a horizontal stage with no further increase in strength. This was termed the ‘critical state’, and the simple relation $\sigma_1 = 3\sigma_3$ suggested itself, as illustrated in Fig. 2.

An extensive recent study by Singh et al. (2011) in Roorkee University involving re-analysis of thousands of reported triaxial tests, including their own testing contributions, has revealed the

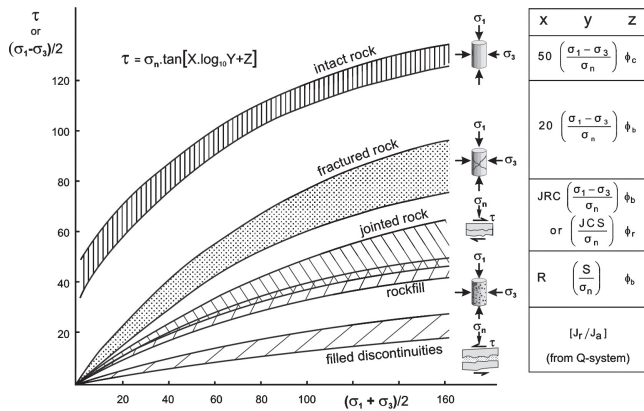


Fig. 1. Simple empiricism, sometimes based on hundreds of test samples, suggested these simple ways to express peak shear strength (τ). Note the general lack of cohesion (Barton, 1976).

astonishing simplicity of the following equality: $\sigma_c \approx \sigma_{3(critical)}$ for the majority of rock types: in other words, the two Mohr circles referred to in Fig. 2 are touching at their circumference. This is at once an 'obvious' result and an elegantly simple result, and heralds a new era of triaxial testing.

The curvature of peak shear strength envelopes is now more correctly described, so that few triaxial tests are required and need only be performed at low confining stress, in order to delineate the whole strength envelope. This simplicity does not of course apply to M-C, nor does it apply to non-linear criteria including H-B, where triaxial tests are required over a wide range of confining stress, in order to correct the envelope, usually to adjust to greater local curvature.

Singh et al. (2011) basically modified the M-C criterion by absorbing the critical state defined in Barton (1976), and then quantifying the necessary deviation from the linear form, using a large body of experimental test data.

Singh and Singh (2012) have developed a similar criterion for the shear strength of rock masses, with σ_c for the rock mass potentially based on the simple formula $5\gamma Q_c^{1/3}$ (where $Q_c = Q\sigma_c/100$ (MPa)). The rock density is γ , and Q is the rock mass quality (Barton et al., 1974), based on six parameters involving relative block size, inter-block friction coefficient and active stress.

3. Shear strength of rock joints

Recent drafts of the ISRM suggested methods for testing rock joints, and widely circulated errors on the Internet and in commercial numerical modelling software, caused the writer to spend some time on the topic of shear strength of rock joints, in his 6th Müller Lecture (Barton, 2011). Problems identified included exaggeration of 'cohesion intercept' in multi-stage testing, and continued use of ϕ_b in place of ϕ_r , thirty-five years after ϕ_r was introduced in a standard equation for shear strength.

Unfortunately, Hoek's downloadable rock mechanics texts and related RockScience software represent the limit of a lot of consulting offices contact with rock mechanics, so they have little knowledge of advances in the field that are not picked up by those who for some reason feel it their duty to feed the internet with 'free' rock mechanics. This is a dangerous and unnecessary state of affairs.

Following the tests on 130 fresh and slightly weathered rock joints (ten of which are shown in Fig. 3), the basic friction ϕ_b was replaced by ϕ_r , which may be several degrees lower. This occurred in 1977, and was unfortunately overlooked/not read by the chief supplier of the Internet with his version of rock mechanics.

Due to the dominance of this 'downloadable rock mechanics', there have been a significant number of incorrectly analyzed rock slopes, and incorrectly back-calculated JRC values in refereed Ph.D. studies, not to mention a number of refereed publications with incorrect formula, due to failure to read outside the downloaded materials.

The reconstructed shearing events shown in Fig. 4 were derived from specific tension fractures with the (two-dimensional, 2D) surface roughness as shown, and displaced and dilated as measured in the specific direct shear tests. These tests on tension fractures were performed in 1968, and represented the forerunner of the non-linear criterion shown in Fig. 4 (#3).

In 1971 (Ph.D. studies of the writer), the 'future' 'JRC' had the value 20, due to the roughness of tension fractures, and the 'future' 'JCS' was merely the uniaxial strength of the (unweathered) model material. For the same reason of lack of weathering, the 'future' ϕ_r at this time was simply ϕ_b .

Fig. 5 illustrates the form of the third strength criterion shown in Fig. 4(top). It will be noted that no cohesion intercept is intended. It will also be noted that subscripts have been added to indicate scale-effect (reduced) values of joint roughness JRC_n and joint wall strength JCS_n . This form is known as the Barton-Bandis criterion. Its effect on strength-displacement modelling is shown later.

The scale-effect correction by Barton and Bandis (1982) is illustrated by three peak shear strength envelopes in Fig. 5. It will be noted that the peak dilation angles vary significantly. This is important when transforming principal stresses to normal and shear stresses that act on a plane. This topic will be discussed later.

Recent drafts and earlier versions of the ISRM suggested methods for shear testing rock joints have suggested multi-stage testing of the same sample, to increase the numbers of test results when there are insufficient samples. Naturally, the first test is recommended performed at low stress to minimize damage. Successive tests are performed at higher normal stress, using the same sample, reset in the 'zero-displacement' position. Since there will be a gradual accumulation of damage, there is already a 'built-in' tendency to reduce friction (and dilation) at higher stress, and therefore to increase the apparent cohesion intercept (if using M-C interpretation). These problems are accentuated if JRC is high, and JCS low and normal stress high in relation to JCS, therefore causing more damage during each test.

A further tendency to rotate the 'peak' strength envelope clockwise (and exaggerate an actually non-existent M-C cohesion) is

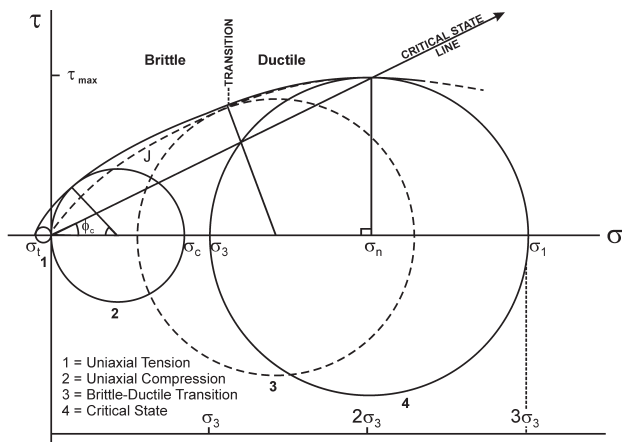


Fig. 2. Critical state line defined by $\sigma_1 = 3\sigma_3$ was suggested by numerous high-pressure triaxial strength tests. Note the chance closeness of the unconfined strength (σ_c) circle to the confining pressure $\sigma_{3(critical)}$ (Barton, 1976). Note that 'J' represents jointed rock. The magnitude of ϕ_c is 26.6° when $\sigma_1 = 3\sigma_3$.

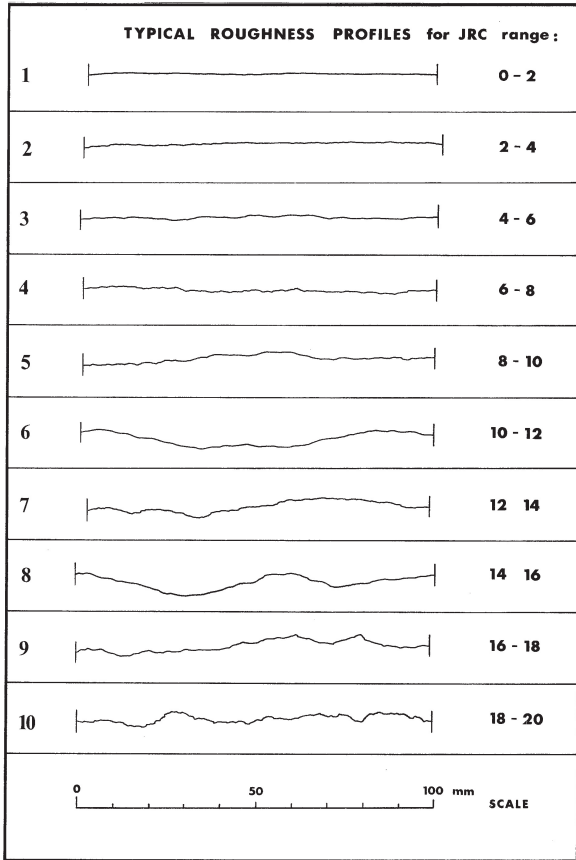
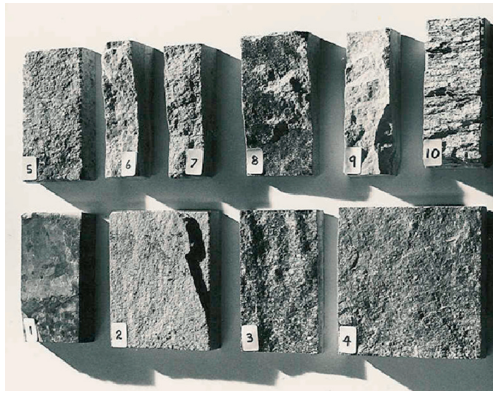


Fig. 3. A simple joint-roughness (JRC) based criterion for peak shear strength. Ten typical samples are shown, together with their roughness profiles. The Barton and Choubey (1977) criterion has the form shown in Fig. 4 (third criterion listed).

the frequent instruction to preload each sample to a higher normal stress. Barton (2007) (following Barton, 1971) showed that this causes over-closure, and higher resulting shear strength, especially in the case of rough joints. We need to be concerned here (extracted from Barton, 2007):

Thermal effects in future nuclear waste repositories may further accentuate over-closure, due to an additional thermal effect: roughness profiles ‘remember’ the warmer/hotter initiation temperature, and fit together better when heated. The rougher joints may remain closed when cooled as they then have some tensile strength and much increased shear strength. Smoother longer joints will then open in preference and disqualify conventional-behaviour based designs. These effects have been seen to compromise expected results of URL (underground research lab) in situ experiments, but are so far

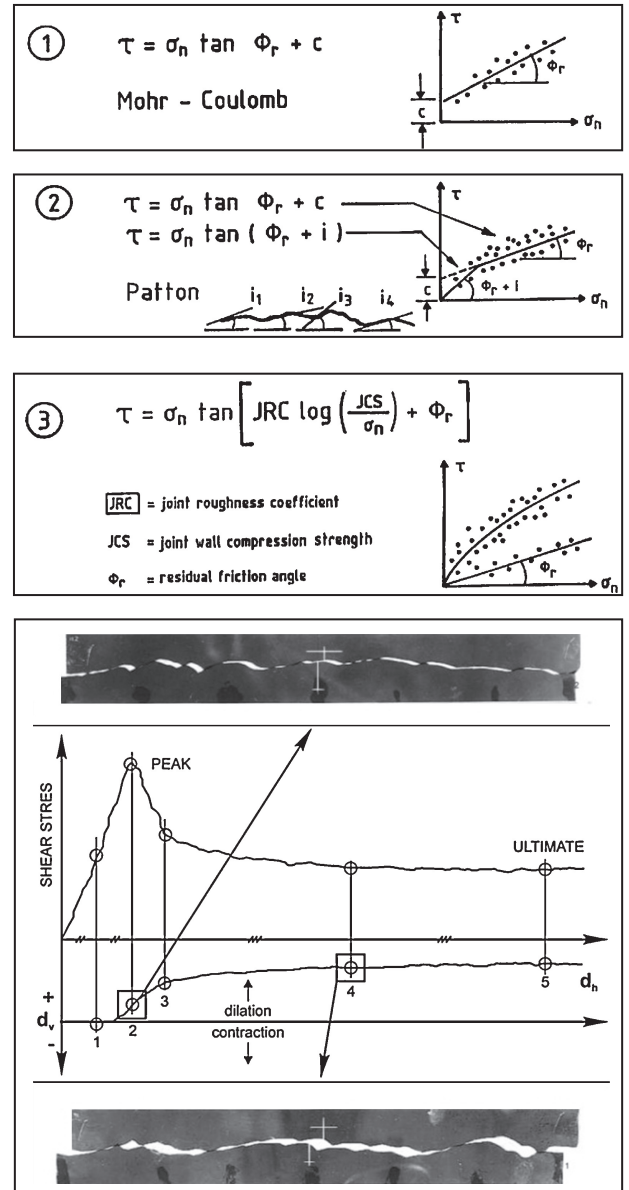
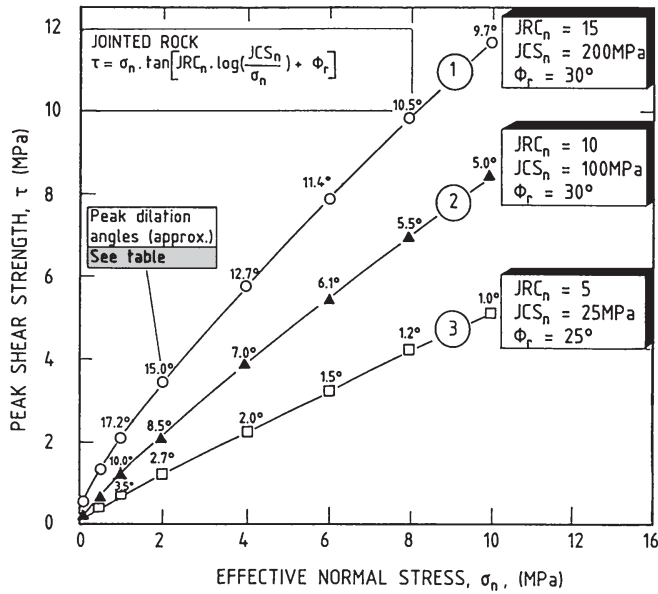


Fig. 4. The (third) non-linear shear strength criterion for rock joints was developed first from (unweathered) tension fractures, and had ϕ_b in place of ϕ_r . The sheared replicas of rough tension fractures are sheared and dilated as tested (Barton, 1971, 1973).

ignored in codes – also in UDEC-BB – and in HLW (high-level waste) design.

The maintenance of the above described multi-stage testing procedures for rock joints has inadvertently prolonged the artificial life support of cohesion, affecting numerical modelling and countless thousands of consultants’ reports and designs.

Some people have of course questioned the use of rock joint ‘cohesion’ in rock slope design, even in large scale open pit design, and ‘to be on the safe side’ they ignore cohesion. This is safe but expensive, as with the above two tendencies to rotate the strength envelope clockwise (increasing ‘cohesion’ and reducing ‘friction’), the resulting ‘safe’ friction angle may be far too conservative, and probably joint continuity is already assumed to be too high.



Estimates of peak dilation angles (d_n°)

Curve no.	Effective normal stress (MPa)								
	0.1	0.5	1.0	2.0	4.0	6.0	8.0	10.0	
1	24.7	19.5	17.2	15.0	12.7	11.4	10.5	9.7	
2	15.0	11.5	10.0	8.5	7.0	6.1	5.5	5.0	
3	6.0	4.2	3.5	2.7	2.0	1.5	1.2	1.0	

Fig. 5. The scale-effect corrected form of the non-linear Barton (1973) strength criterion, from Barton and Bandis (1982), following modification with ϕ_r by Barton and Choubey (1977).

4. Pre-peak, post-peak shear strength

Fig. 6 illustrates the strength-deformation-stiffness model used in the Barton–Bandis constitutive law for rock joints. Friction is mobilized just before roughness and dilation are mobilized. After peak shear strength, JRC (and JRC_n) is gradually destroyed. One should note the ‘impossibility’ of reaching residual strength. The magnitude of ϕ_r is illustrated in Fig. 7. This important parameter can be estimated by the index tests shown in Fig. 8. This figure shows a series of index tests for characterizing the strength parameters needed to explain the non-linearity and scale-dependence of shear strength. Tilt tests are shown in Fig. 9.

5. Shear strength of rockfill interfaces

Fig. 1 showed that there were similarities between the shear strength of rockfill and that of rock joints. This is because they both have ‘points in contact’, as shown in Fig. 10, i.e. highly stressed contacting asperities or opposing stones. In fact these contacting points may be close to their crushing strength, such that similar shear strength equations apply:

- (1) $\tau/\sigma_n = \tan[JRC \cdot \log_{10}(JCS/\sigma_n) + \phi_r]$ applies to rock joints.
- (2) $\tau/\sigma_n = \tan[R \cdot \log_{10}(S/\sigma_n) + \phi_b]$ applies to rockfill.
- (3) $\tau/\sigma_n = \tan[JRC \cdot \log_{10}(S/\sigma_n) + \phi_r]$ might apply to interfaces.

The equation to be used for the interface will depend on whether there is ‘JRC’ control, or ‘R’ control. This distinction is described, and illustrated later (Fig. 11).

Because some dam sites in glaciated mountainous countries like Norway, Switzerland, Austria have insufficient foundation roughness to prevent preferential shearing along the rockfill/rock foundation interface, artificial ‘trenching’ is needed. Various scales

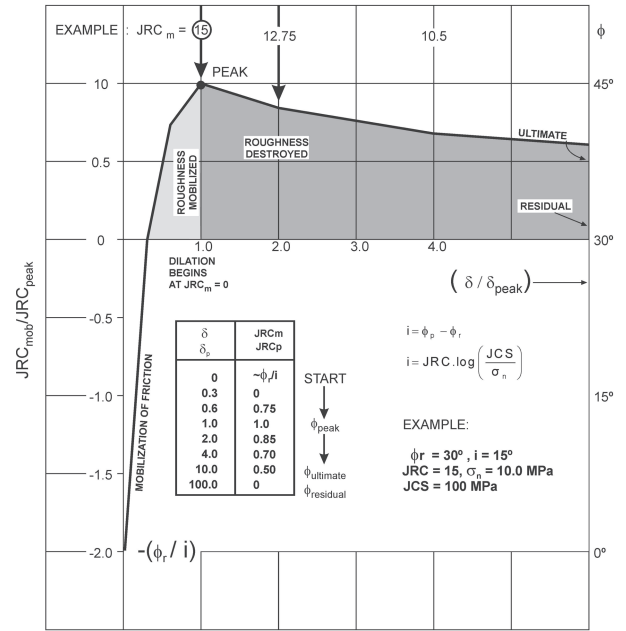


Fig. 6. The $JRC_{mobilized}$ concept developed by Barton (1982) allows the modelling of strength-deformation-dilation trends, as shown in Fig. 7. Note that ‘i’ changes with the normal stress.

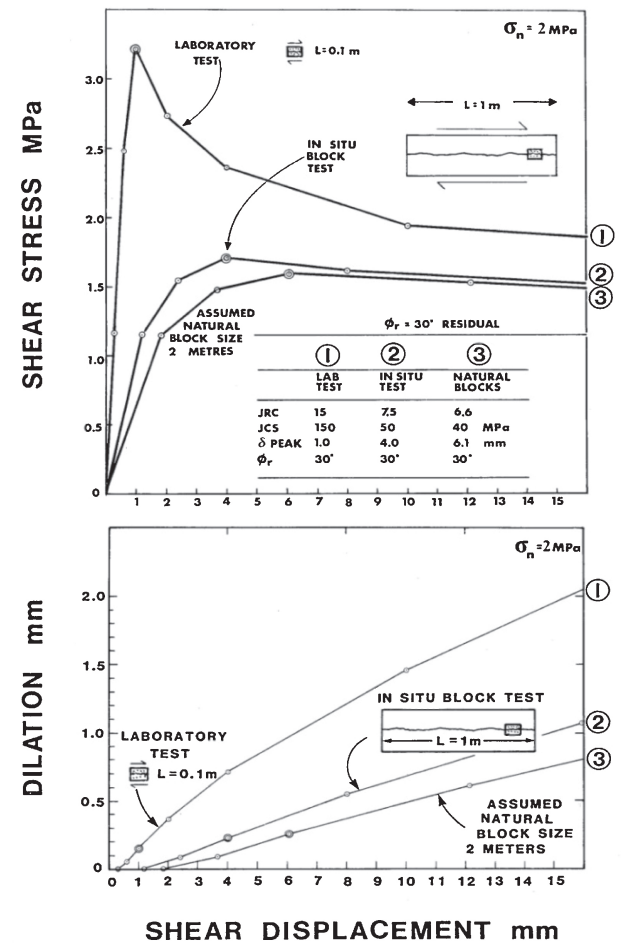


Fig. 7. With scale effects caused by increasing block size accounted for (see input data in the inset), we see that laboratory testing, especially of rough joints, may need a strong adjustment (down-scaling) for application in design (Barton, 1982).

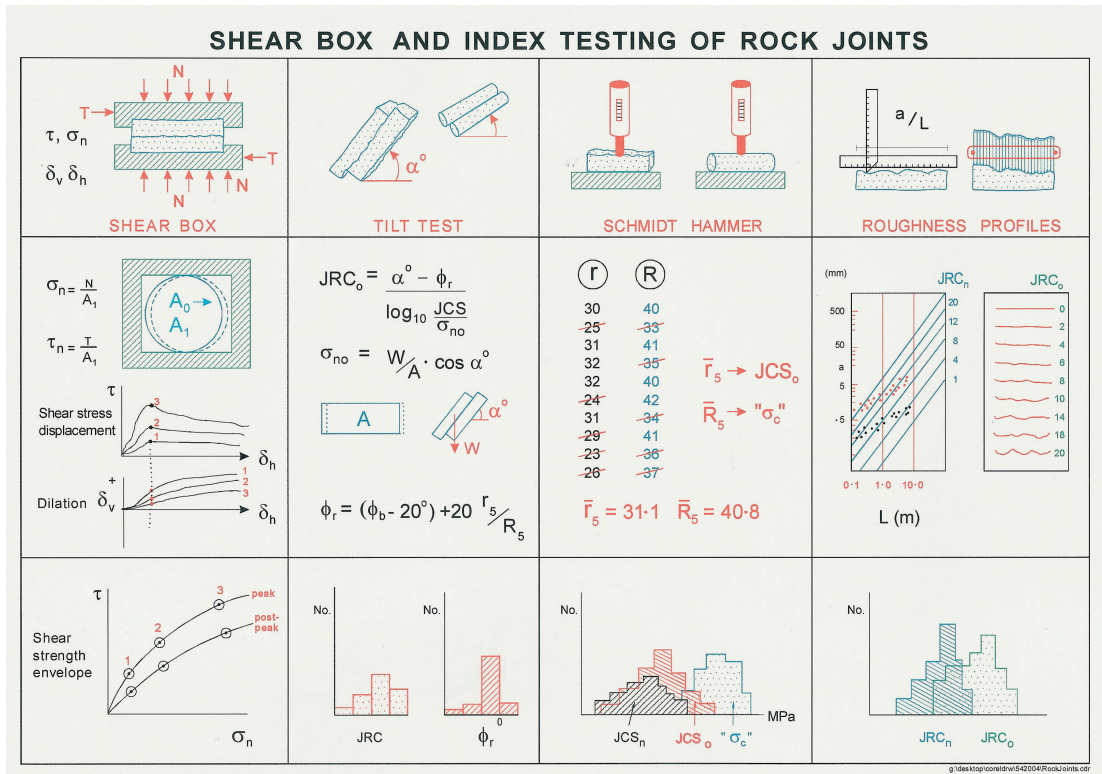


Fig. 8. Direct shear testing and typical results are shown in the first (left-hand) column. Tilt tests for JRC and ϕ_b (and conversion to ϕ_r) are shown in the second column, (also see Fig. 9), and Schmidt hammer testing for r (weathered joint) and R (unweathered core stick) are shown in the third column. More direct roughness (JRC) measurement is shown in the fourth column, using the amplitude/length (a/L) method, or brush-gauge recording. The a/L method is simple to interpret.

of investigation of interface strength have been published. These were analyzed in unpublished research performed by the author, and can be summarized by the data points plotted in Fig. 12.

Fig. 13 illustrates real examples of these two categories of shearing, in which the 'weakest link' determines the mode of sliding: whether the interface is smooth enough and the particles big enough to prevent good interlock (JRC-controlled), or the opposite R-controlled behaviour, with preferential failure within the rockfill.

6. Numerical modelling of rock masses

It has been claimed – correctly – that rock masses are the single most complex of engineering materials utilized by man. We utilize

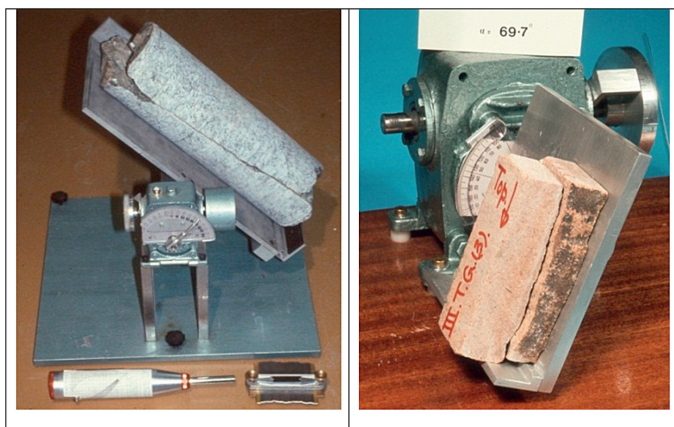


Fig. 9. Tilt testing of large diameter core and sawn blocks. Note Schmidt hammer, and roughness-measurement brush gauge.

rock masses for purposes as diverse as road, rail and water transport tunnels, dam site location, oil and gas storage, food storage and sports facilities in caverns, and we are heading for final disposal of high-level nuclear waste.

The complexity may be due to variable jointing, clay-filled discontinuities, fault zones, anisotropic properties, and dramatic

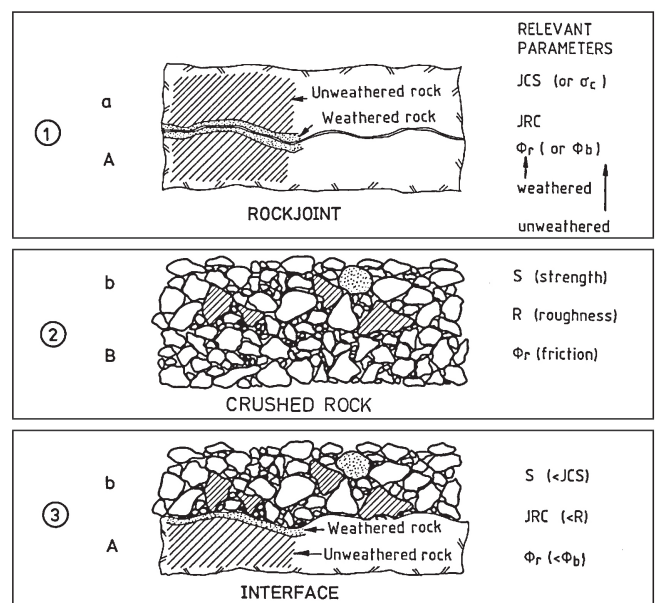


Fig. 10. Peak shear strength estimates for three categories of asperity or point-to-point contact. As seen in Fig. 11, it is possible to test as-built rockfill, if the tilt-testing box is of large enough dimensions to take the compacted rockfill, from the next 'lift'.

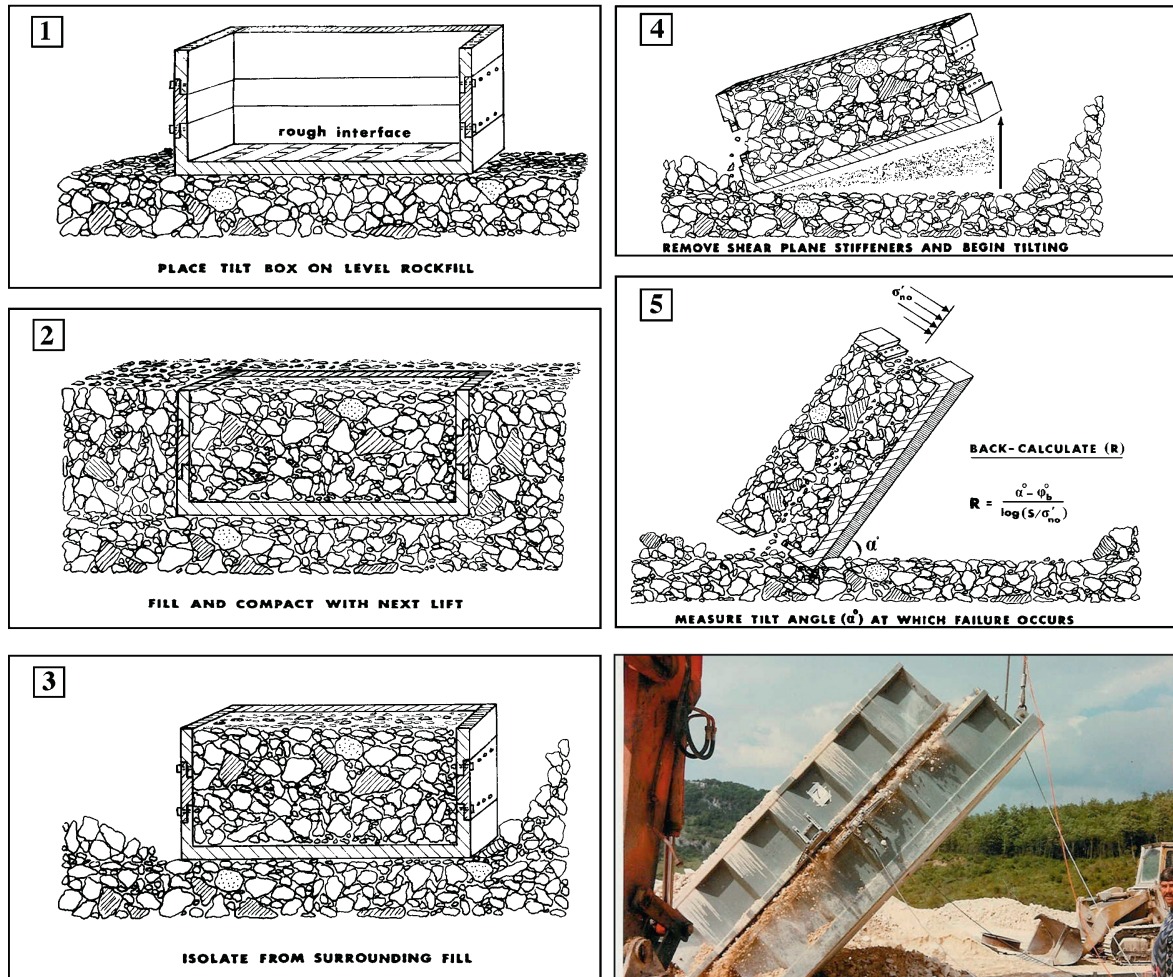


Fig. 11. Tilt testing of as-built rockfill, as suggested in Barton and Kjærnsli (1981), with performance of ten tests at a rockfill dam in Italy. The tilt-shear box is 5 m × 2 m × 2 m.

water inrush and rock-bursting stress problems. Nevertheless we have to make some attempt to represent this complexity in models. Two contrasting approaches (to a simple case) are shown in Fig. 14.

When modelling a rock mass in a 2D representation, as illustrated, it is clear that deformation modulus, Poisson's ratio, shear and tensile strengths, and density will figure as a minimum in both models. In the case of the additional representation of the jointing, one will in the case of UDEC-BB also specify values of JRC, JCS and φ_r for the different joint sets, paying attention also to the spacing of cross-joints so that relevant ranges of block sizes L_n are specified, in relation to the usually smaller scale L_0 size of blocks or core pieces tested when characterizing the site (L_0 and L_n are the lab-scale and in situ scale block sizes).

It is clear that the shear strength of the jointed model will be dominated by 'the weakness' of its jointing. Equivalent continuum values of shear strength will be assigned in the case of the continuum representation. It is here that the problems begin. The limitations of M-C, H-B and 'c plus $\sigma_n \tan \varphi$ ' are likely to be observed. Attempts to model 'break-out' phenomena such as those illustrated in Fig. 15 are not especially successful with standard M-C or H-B failure criteria, because the *actual phenomena* are not following our long-standing belief in 'c plus $\sigma_n \tan \varphi$ '. The reality is degradation of cohesion at small strain and mobilization of friction (first towards peak, then towards residual) which occur at larger strain. We register closure or squeezing, and also can measure it, as an *apparent radial strain*. In reality, it may be a tangential strain-related failure phenomenon.

The very important findings of Hajiabdolmajid et al. (2000) are summarized briefly by means of the six figures assembled in Fig. 15. The demonstrated shortcomings of continuum modelling with 'c plus $\sigma_n \tan \varphi$ ' shear strength assumptions should have alerted our profession for change already twelve years ago, but deep-seated beliefs or habits are traditionally hard to change (Barton, 2011).

Rock masses actually follow an even more complex progression to failure, as suggested in Barton and Pandey (2011), who recently demonstrated the application of a similar 'c then $\sigma_n \tan \varphi$ ' modelling approach, but applied it in FLAC^{3D}, for investigating the behaviour of multiple mine-stopes in India. A further break with convention was the application of peak 'c' and peak ' φ ' estimates that were derived directly from mine-logged Q-parameters, using the CC (cohesive component) and FC (frictional component) parameters suggested in Barton (2002). For this method, an estimate of UCS (uniaxial compressive strength) is required, as CC and FC are derived from separate 'halves' of the formula for $Q_c = Q\sigma_c/100$ (The Q formula is shown below Fig. 16, where empirically derived $Q_c - V_p - M$ inter-relationships are shown).

The two or three classes of discontinuities (natural and induced) involved in *pre-peak* and *post-peak* rock mass failure will tend to have quite different sets of shear strength properties. For instance, the *new stress-induced failure surfaces*, if described with JRC, JCS and φ_r , might have respective numbers (at small scale) like 18–22, 100–150 MPa and 30°–32° (i.e. rough and unweathered and strongly dilatant), compared to perhaps 4–8, 50–100 MPa and 27°–29° for potential joint sets, or perhaps $J_r/J_a = (1-2)/4$ for any clay

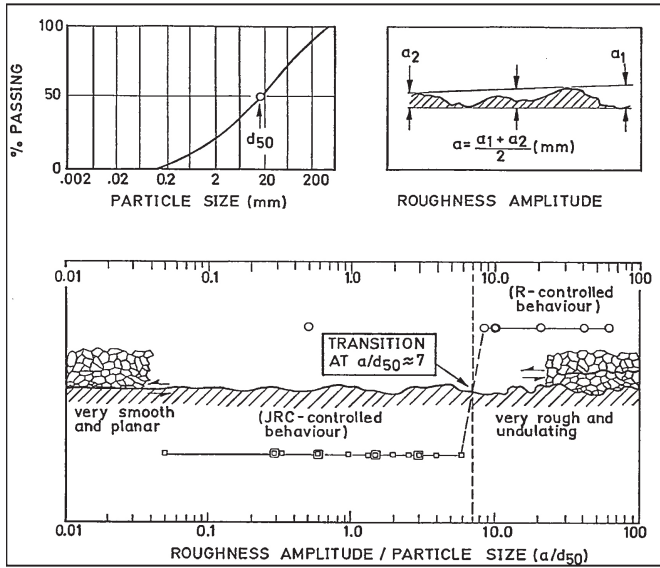


Fig. 12. The results of interface/rockfill and interface/sand (and gravel) direct shear tests can be separated by means of the ratio a/d_{50} , into R-controlled and JRC-controlled categories.

coated discontinuities, that might also be involved in the post-peak shear strength behaviour of the rock mass. Shear strength description using J_r/J_a is from the Q-system (Barton et al., 1974; Barton, 2002), which is shown in Fig. A.1. in Appendix A.

The dilatancy obviously reduces strongly between these three groups of discontinuities. Furthermore, each of the above has the features that begin to resist shearing at considerably larger strains/deformations than is the case for the also strongly dilatant failure of the ‘intact bridges’. Why therefore are we adding ‘ c and $\sigma_n \tan \phi$ ’ in ‘continuum’ models, making them even poorer representations of the strain-and-process-sensitive reality?



Fig. 13. Four examples of a/d_{50} that demonstrate either preference for interface sliding or preference for internal shearing in the rockfill. This can be checked (at low stress) by tilt-testing.

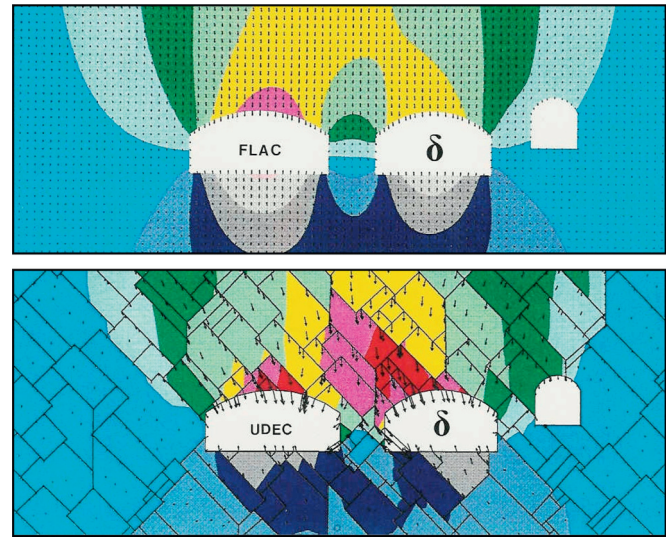


Fig. 14. Continuum and discontinuum modelling approaches to the representation of a rather uncomplicated, though anisotropic rock mass. The increased richness and reality of representing the potential behaviour of jointing, even if exaggerated in 2D, is clear to see.

Input data obtained via Hoek and Brown and GSI ($GSI = RMR - 5$) formulations that obviously ignore such complexity and reality, since not representing rock fracture and joint strength, nevertheless consist of remarkably complex algebra (e.g. Table 1) in comparison to the more transparent formulae for discontinuum codes, where JRC_0 , JCS_0 , ϕ_r , L_0 and L_n and use of Barton–Bandis scaling equations are sufficient to develop the key joint strength and joint stiffness estimates.

A demonstration of the simpler, Q-based continuum-model ‘cohesive component’ (CC) and ‘frictional component’ (FC) for a variety of rock mass characteristics is given in Table 2. Low FC needs more bolting, while low CC needs more shotcrete, even local concrete linings. These are semi-empirically based ‘halves’ of the Q-formula, which seem to be realistic.

These much simpler Q-based estimates have the advantage of not requiring software for their calculation – they already exist in the Q-parameter logging data, and the effect of changed conditions such as clay-fillings, or an additional joint set can be visualized immediately. This is not the case with Eqs. (2) and (4) in Table 1.

An important part of the verification of this mine stope modelling by Pandey, described in Barton and Pandey (2011), was the comparison of the modelling results with the deformations actually

Table 1

The remarkable complexity of the algebra for estimating c' and ϕ' with Hoek–Brown GSI-based formulations is contrasted with the simplicity of equations derived by ‘splitting’ the existing Q_c formula into two parts, as described in Barton (2002) ($Q_c = Q\sigma_c/100$, with σ_c expressed in MPa).

Expression	Origin
$\phi' \approx \tan^{-1} \left(\frac{J_r}{J_a} \times \frac{J_w}{1} \right)$	(1) FC from Q
$\phi' = a \sin \left[\frac{6am_b(s + m_b\sigma'_{3n})^{a-1}}{2(1+a)(2+a) + 6am_b(s + m_b\sigma'_{3n})^{a-1}} \right]$	(2) From GSI
$c' \approx \left(\frac{RQD}{J_n} \times \frac{1}{SRF} \times \frac{\sigma_c}{100} \right)$	(3) CC from Q
$c' = \frac{\sigma_{ci} [(1+2a)s + (1-a)m_b\sigma'_{3n}] (s + m_b\sigma'_{3n})^{a-1}}{(1+u)(2+a)\sqrt{1 + [6am_b(s + m_b\sigma'_{3n})^{a-1}]/[(1+a)(2+a)]}}$	(4) From GSI

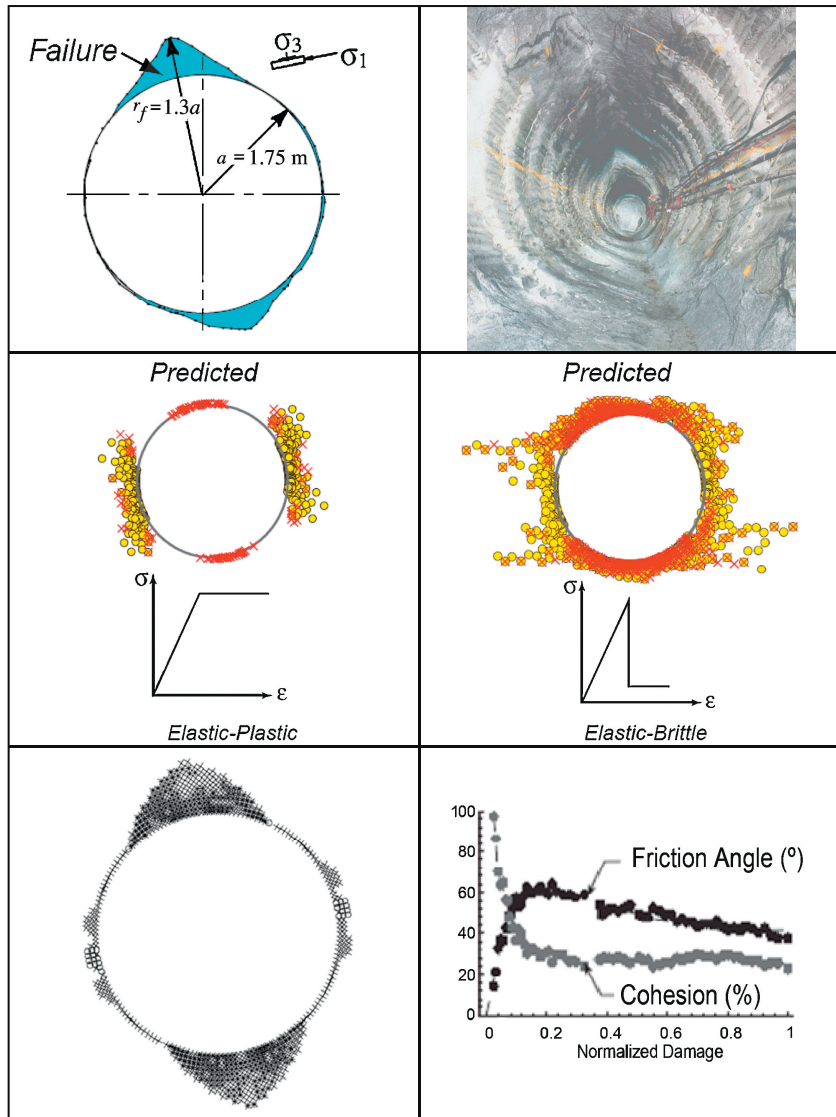


Fig. 15. Top: The Canadian URL mine-by break-out that developed when excavating by line-drilling, in response to the obliquely acting anisotropic stresses. This is followed by an important demonstration of *unsuccessful* modelling by ‘classical methods’ given by Hajiabdolmajid et al. (2000). They followed this with a *more realistic* degradation of cohesion and mobilization of friction in FLAC.

measured with pre-mining pre-installed MPBX (extensometer) arrays, and cross referencing with empirical formulations for deformation, which are shown in Fig. 17. All three sources of deformation (measured, modelled, empirical) showed good agreement (see Barton and Pandey, 2011).

Recent reviews of pre-excavation modelling for cavern design, and cavern performance reviews for a major metro constructor in Asia, suggest that it is wise to consult these two simple equations, when deliberating over the reality (or not) of numerical models. It is

the experience of the writer that UDEC-MC and UDEC-BB modellers often exaggerate the continuity of modelled jointing (because this is easier than drawing a more representative image of the less-continuous jointing, and digitizing the latter).

A common result of UDEC models with exaggerated joint continuity is that modelled deformations may be at least 10× those which are subsequently measured, and support needs have therefore been exaggerated, because of the artificial deformations. The common opinion expressed by the a priori modellers is that the

Table 2
Illustration of parameters CC (MPa) and FC (°) for a declining sequence of rock mass qualities, with simultaneously reducing σ_c (MPa). Estimates of V_p (km/s) and E_m (GPa) are from Fig. 16, whose derivation was described in Barton (2002).

RQD	J_n	J_r	J_a	J_w	SRF	Q	σ_c (MPa)	Q_c	FC (°)	CC (MPa)	V_p (km/s)	E_m (GPa)
100	2	2	1	1	1	100	100	100	63	50	5.5	44
90	9	1	1	1	1	10	100	10	45	10	4.5	22
60	12	1.5	2	0.66	1	2.5	50	1.25	26	2.5	3.6	11
30	15	1	4	0.66	2.5	0.1	33	0.04	9	0.3	2.1	3.5

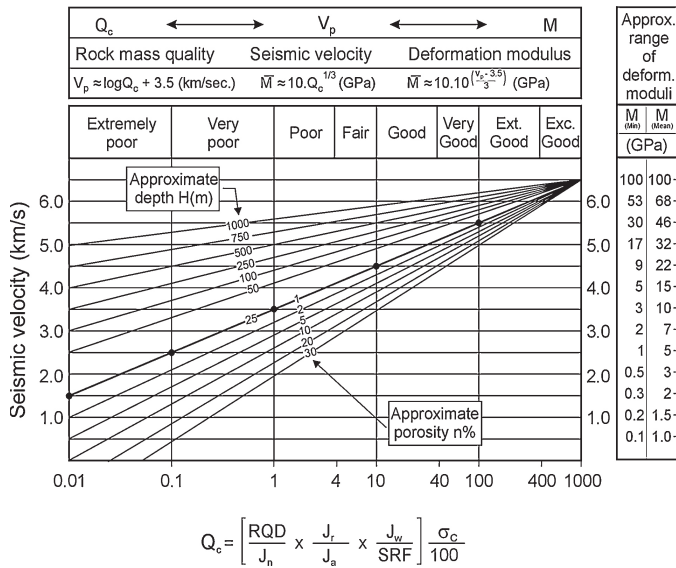


Fig. 16. Empirical relationships between Q values (with parameters as shown) and P-wave velocity and (static) deformation modulus M . Note corrections for increased depth or stress level, which should be applied in numerical models when significant depth variation is to be modelled (Barton, 2002).

Table 3

Empirical equations linking tunnel or cavern deformation to Q -value (from Barton, 2002). In the top equation $SPAN$ = meters (as in the vertical axes of Fig. 17). In the bottom equation $SPAN$ = mm. Both Δ and Δ_v are in millimeters. Vertical stress and compressive strength must have consistent units, e.g. MPa.

Expression	Note
$\Delta = \frac{SPAN}{Q}$	Central trend of all data: approx
$\Delta_v = \frac{SPAN}{100Q} \sqrt{\frac{\sigma_v}{\sigma_c}}$	More accurate estimate

a posteriori Q -system based support recommendation is not adequate. Of course they are incorrect.

In fact, when the caverns are finally constructed, they may be almost self-supporting, and certainly could be permanently supported with single-shell shotcrete and (corrosion protected) rock bolting: $B+S(fr)$, which is termed NMT to distinguish it from the much more expensive double-shell NATM (with final concrete lining).

Note that at the record-breaking 62 m span Gjøvik cavern, excavated in fresh to slightly weathered grey and red gneiss, with most frequent $Q_{core} = 10$, $Q_{cavern\ arch} = 12$, the equations show 6–7 mm, while the UDEC modelling (with realistic non-continuous jointing) showed 7–8 mm, and the MPBX (plus surface levelling) showed 7–8 mm. This was a single-shell NMT-concept drained cavern, and concrete lining was never considered (Barton et al., 1994).

7. Fundamental geotechnical error?

This paper will be concluded with a subject that has been little discussed and little publicized (Ch. 16, Barton, 2006). It appears to go beyond the more common distinction that we make between constant normal stress and constant normal stiffness shear testing of rock joints.

The subject of concern is the transformation of stress from a principal (2D) stress state of σ_1 and σ_2 to an inclined joint, fault or failure plane, to derive the commonly required shear and normal stress components τ and σ_n . If the surface onto which stress is to be transformed does not dilate, which might be the case with a (residual-strength) fault or clay-filled discontinuity, then the assumption of co-axial or co-planar stress and strain is no doubt valid.

If on the other hand dilation is involved, then stress and strain are no longer co-axial. In fact the plane onto which stress is to be transferred should even be an imaginary plane. Any non-planar rock joints and any failure planes through dense sand or through over-consolidated clay or through compacted rockfill, are neither imaginary nor non-dilatant in nature.

This problem nearly caused a rock mechanics related injury, when Bakhtar and Barton (1984) were attempting to biaxially shear diagonally fractured 1 m³ samples of rock, hydrostone and concrete. The experimental set-up and various index tests are shown in Fig. 18. The sample preparation was unusual because of principal stress (σ_1) driven controlled-speed tension fracturing (see triangular flat-jacks in top-left photo). This allowed fractures to be formed in a controlled manner. Fig. 19 shows the stress application and related assumptions (presented in three stages).

The rock mechanics near-injury occurred when a (σ_1 -applying) flatjack burst at 28 MPa, damaging the laboratory walls and nearly injuring the writer who was approaching to see ‘what the problem was’. The sample illustrated in Fig. 18 (with photographer’s shoes) was transformed into ejected slabs and ejected high-pressure oil, damaging pictures on the walls, as a result of the dramatic flatjack burst.

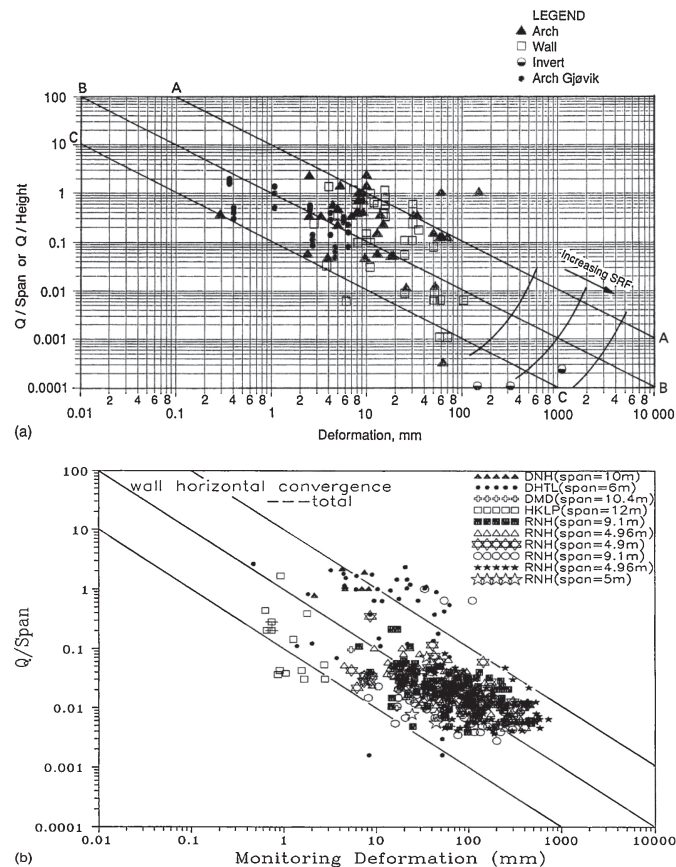


Fig. 17. Two complementary figures (top figure from Barton et al., 1994), showing a total of many hundreds of tunnel monitoring data. Their source is given in Barton (2002). The central (very approximate) data trend can be described by the simplest equation that is possible in rock engineering. See Table 3, which also shows a more accurate version for checking the probable validity (or need for adjustment of joint representation) in numerical model results.

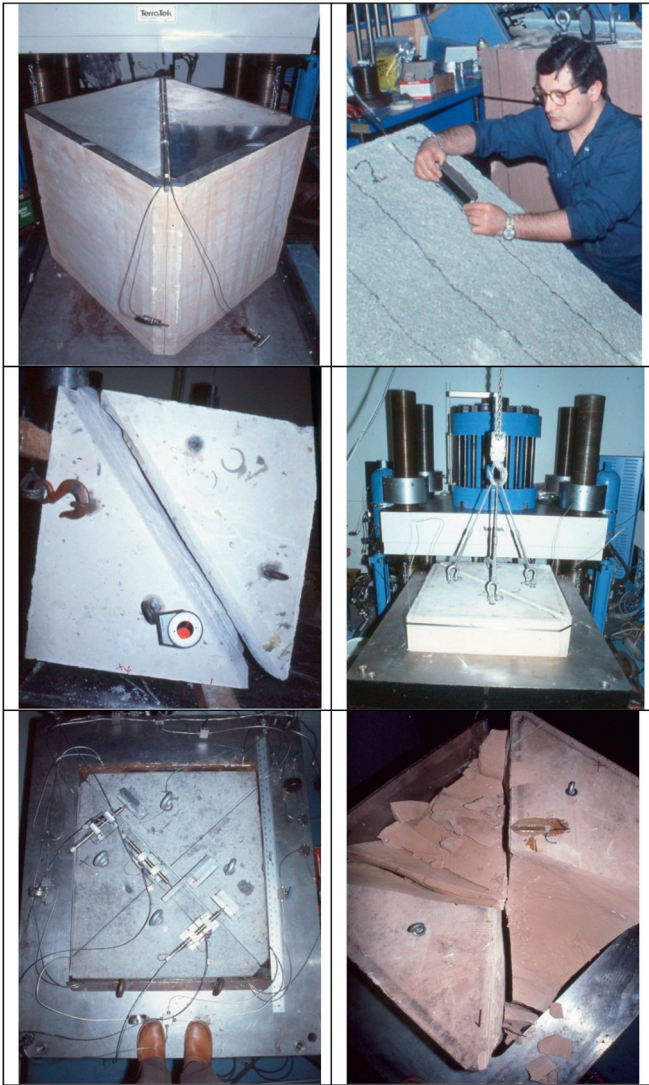


Fig. 18. Sample preparation, roughness profiling by TerraTek colleague Khosrow Bakhtar, tilt testing (at 1 m³ scale), lowering lightly clamped sample into test frame, LVDT instrumentation, and (a rare) sheared sample of an undulating fracture in sandstone. These 1.3 m long tension fractures displayed tilt angles varying from 52° to 70°, and large-scale ($L_n = 1.3$ m) joint roughness coefficients varying from 4.2 to 10.7.

The conventional and dilation corrected stress transformation equations can be written as

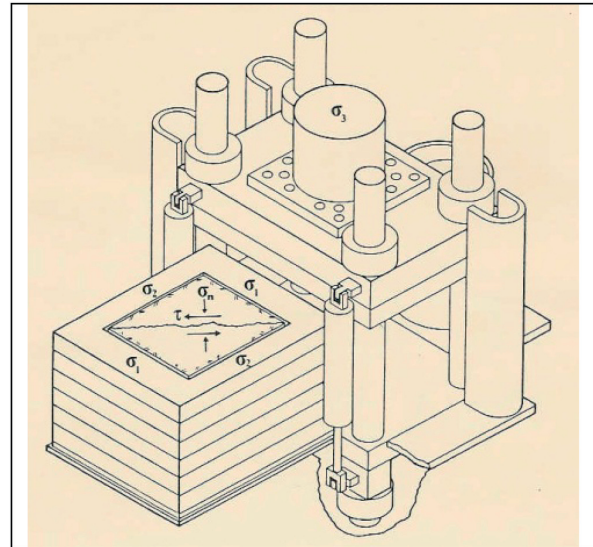
$$\left. \begin{aligned} \sigma_n &= \frac{1}{2}(\sigma_1 + \sigma_2) - \frac{1}{2}(\sigma_1 - \sigma_2) \cos(2\beta) \\ \tau &= \frac{1}{2}(\sigma_1 - \sigma_2) \sin(2\beta) \end{aligned} \right\} \quad (5)$$

$$\left. \begin{aligned} \sigma_n &= \frac{1}{2}(\sigma_1 + \sigma_2) - \frac{1}{2}(\sigma_1 - \sigma_2) \cos[2(\beta + d_{n, mob})] \\ \tau &= \frac{1}{2}(\sigma_1 - \sigma_2) \sin[2(\beta + d_{n, mob})] \end{aligned} \right\} \quad (6)$$

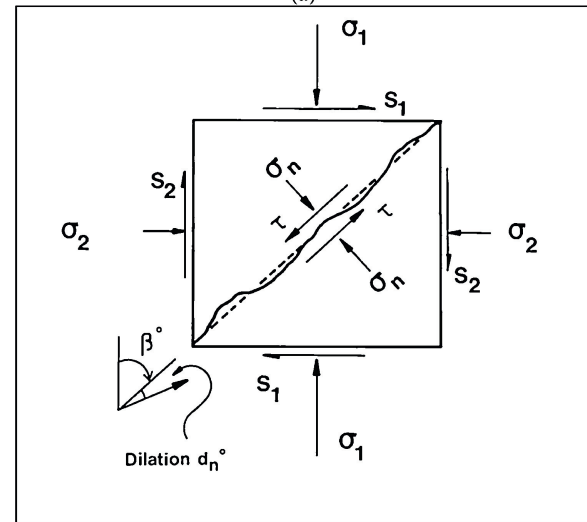
where angle β is the acute angle between the principal stress σ_1 and the joint or failure plane.

The peak dilation angle and mobilized dilation angle can be written as

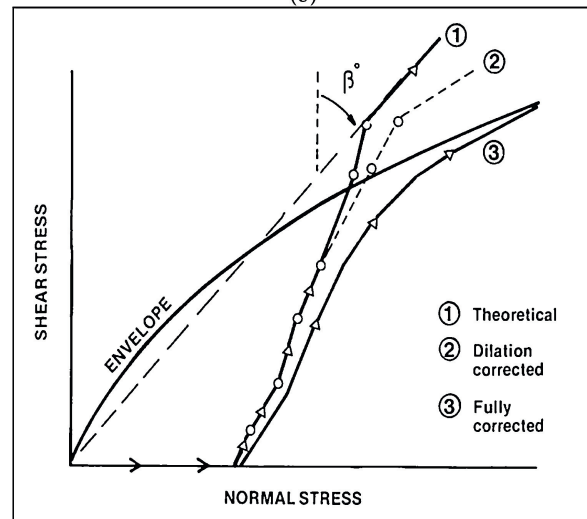
$$d_{n(peak)}^0 = \frac{1}{2} JRC_{(peak)} \log_{10} \left(\frac{JCS}{\sigma_n} \right) \quad (7)$$



(a)



(b)



(c)

Fig. 19. (a) Test set-up, (b) stress transformation and (c) corrections for out-of-plane dilation and boundary friction (Note: greased double-Teflon sheets and pairs of stainless-steel 0–30 MPa flatjacks were used on all four boundaries).

An estimate of the mobilized dilation angle $d_{n(\text{mob})}^0$ for adding to the joint angle β , is as follows:

$$d_{n(\text{mob})}^0 = \frac{1}{2} JRC_{(\text{mob})} \log_{10} \left(\frac{JCS}{\sigma'_n} \right) \quad (8)$$

The dimensionless model for mobilization of roughness ($JRC_{(\text{mob})}$) was shown in Fig. 6.

8. Conclusions

- (1) Recognition of the need to improve the M-C and other (non-linear) shear strength criteria for the intact strength of rock has led researchers at the University of Roorkee to incorporate a simple critical state concept for rock, and thereby delineate the necessary deviation from linear M-C criterion, in order to model correct curvature of the strength envelope.
- (2) The critical confining pressure $\sigma_{3(\text{critical})}$ required to achieve maximum possible shear strength, where the Mohr envelope becomes horizontal, is approximately the same as the UCS for the case of most rock types. Thus $\sigma_{1\text{maximum}} = 3\sigma_{3(\text{critical})} \approx 3\sigma_c$. This is a surprisingly simple, though not illogical result. The result is that triaxial tests only need to be performed at low confining pressures, in order to give the complete strength envelope. This is not the case for M-C or H-B criteria.
- (3) Rock joints have had a valid non-linear strength criterion for 35 years, but tradition dies hard, and linear M-C extrapolations of test data, continue to deceive many into thinking that rock joints have cohesive strength. The reality is high friction, no cohesion and strong dilation at low stress.
- (4) Current multi-stage testing routines for rock joints tend to exaggerate cohesion and reduce friction. If the apparent cohesion intercept is ignored, the ultra-conservative friction angle makes for unnecessarily expensive rock slope design.
- (5) Incorrect downloadable 'internet-age' rock mechanics has introduced an error in slope stability analyses and in research concerning the joint roughness term JRC. This is because the 35 years-old change to the residual friction angle φ_r in place of the unweathered basic friction angle φ_b was overlooked, when 'reproducing' the writer's shear strength criteria.
- (6) The error of recommending φ_b in place of φ_r may represent several degrees different strengths if joints are weathered, and results in incorrect back-calculated JRC values. This error, though now corrected, continues to affect research in universities, and publications continue to propagate this internet-age error, even in professor-monitored research and peer-reviewed publications.
- (7) Rockfill placed on a rock foundation that is smoothed by glaciation may show preferential sliding along this interface. This is termed JRC-controlled behaviour. If the ratio a/d_{50} of roughness amplitude and particle (stone) size exceeds about 7, experimental results suggest that behaviour will be R-controlled with preferential shearing through the rockfill instead.
- (8) R and S replace JRC and JCS in the strength criterion for rockfill. Large-scale tilt tests can be performed with as-built compacted rockfill, using a special 'excavatable' shear box.
- (9) Rock masses are generally jointed, and may be faulted, and are generally anisotropic. Nevertheless those a little external to the better educated rock mechanics communities are encouraged to model with isotropic continuum models, and are able to produce colourful and exaggerated plastic zones that adversely influence bolt-length decisions in the case of tunnel support.
- (10) There is a fundamental question mark hanging over the assumed validity of adding c and $\sigma \tan\varphi$ when trying to describe the continuum-based shear strength of rock masses. For almost 50 years since the time of Müller (1966), it has been recognized that cohesion (if existing) is broken at small strain, while friction is mobilized at much larger strain and is the remaining shear strength if displacement continues.
- (11) An alternative strength criterion introduced in Canadian research in about 2000, involves the degradation of cohesion followed by the mobilization of friction. This results in a much better fit to observations of stress-induced failure than M-C or H-B ' c plus $\sigma \tan\varphi$ ' convention, whether linear or non-linear.
- (12) Recently the ' c then $\sigma \tan\varphi$ ' approach was adopted with a new twist: namely the estimation of c and φ from separates halves of the equation for Q . The cohesive component CC and the frictional component FC appear to have been hiding in the empirically based Q-formulation, since the addition of UCS: giving the form $Q_c = Q\sigma_c/100$. Low CC requires more shotcrete, low FC requires more bolting. A semi-empirical origin is suggested, as Q-parameter ratings were adjusted in response to shotcrete and bolting needs described in the 200-plus 1974 case records.
- (13) Numerical modelling with the discrete addition of rock joints in UDEC and 3DEC represents a big step in the direction of more realistic modelling of excavation effects in rock masses, for the purpose of deformation prediction and support design.
- (14) There is however a pitfall in distinct element (jointed) modelling because many modellers appear to exaggerate joint continuity. This is presumably done because it involves less work. It is more time-consuming to create models with more geologically realistic jointing of generally reduced continuity with depth, unless sedimentary rock remains at depth.
- (15) Exaggerating joint continuity, especially in 2D UDEC models, may cause at least a ten-times exaggeration of deformation in comparison to measured results of e.g. cavern deformation response. It is wise to check numerical model predictions of displacement with empirical Q-based formulae, which are based on hundreds of measurements in tunnels and rock caverns.
- (16) Stress transformation of principal stresses onto an inclined geologic plane or potential failure plane that dilates during shearing, has already violated three of the assumptions of the theory: the plane should be imaginary and it should not shear or dilate.
- (17) Many geotechnical materials dilate during shear: non-planar rock joints, compacted rockfill, dense sand, over-consolidated clay. Large-scale experiments with biaxial testing of rock joints or fractures suggest the need to add a mobilized dilation angle into the stress transformation equations. Measured strength then corresponds to this modified stress transformation.

Acknowledgements

The author would like to thank the Editor for his expert assistance in the production of this paper.

Appendix A.

See Fig. A.1.

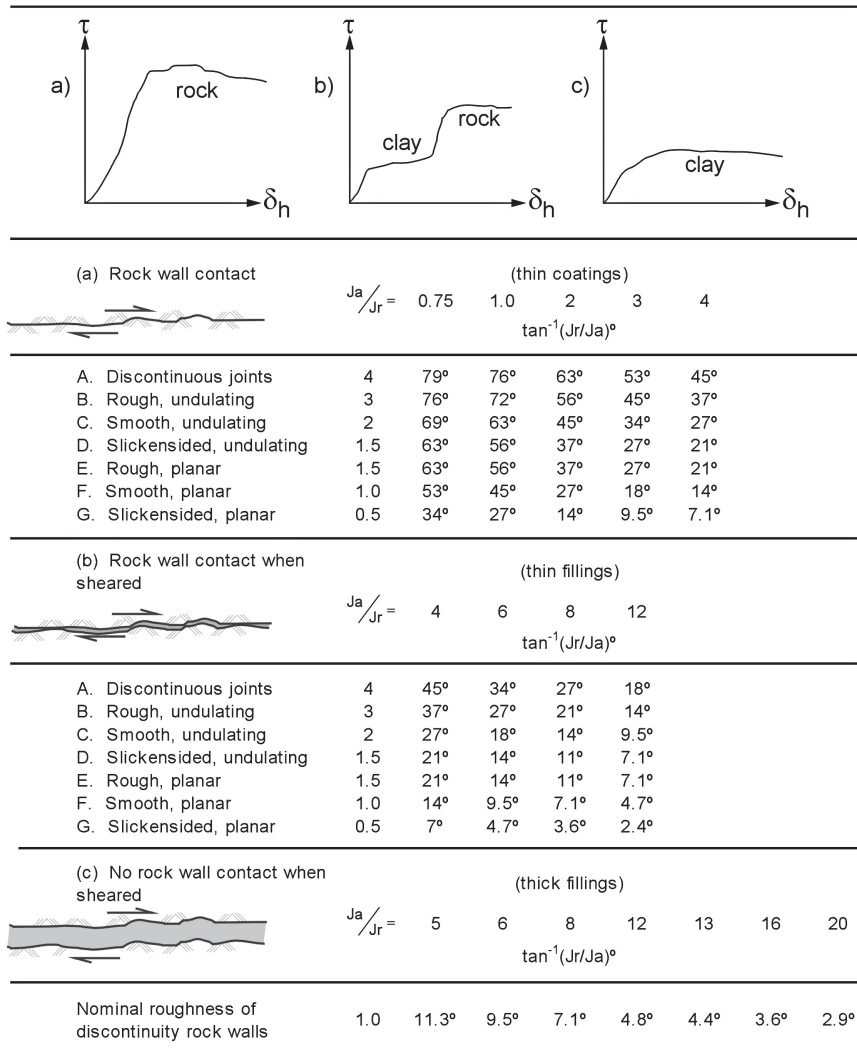


Fig. A.1. Shear strength description using J_r/J_a from the Q-system (Barton et al., 1974; Barton, 2002).

References

Bakhtar K, Barton N. Large scale static and dynamic friction experiments. In: Proceedings of the 25th US rock mechanics symposium. Illinois: Northwestern University; 1984. p. 139–70.

Barton N. A model study of the behaviour of steep excavated rock slopes. London: University of London; 1971. PhD Thesis.

Barton N. Review of a new shear strength criterion for rock joints. Engineering Geology 1973;7(4):287–332.

Barton N, Lien R, Lunde J. Engineering classification of rock masses for the design of tunnel support. Rock Mechanics 1974;6(4):189–236.

Barton N. The shear strength of rock and rock joints. International Journal of Rock Mechanics and Mining Sciences and Geomechanics Abstracts 1976;13(9):255–79.

Barton N, Choubey V. The shear strength of rock joints in theory and practice. Rock Mechanics 1977;10(1/2):1–54.

Barton N, Kjærnsli B. Shear strength of rockfill. Journal of the Geotechnical Engineering Division 1981;107(GT7):873–91.

Barton N. Modelling rock joint behaviour from in situ block tests: implications for nuclear waste repository design. Office of Nuclear Waste Isolation ONWI-308: Columbus, OH; 1982. p. 96.

Barton N, Bandis S. Effects of block size on the shear behaviour of jointed rock. In: Keynote lecture. Proceedings of the 23rd US symposium on rock mechanics; 1982. p. 739–60.

Barton N, By TL, Chryssanthakis P, Tunbridge L, Kristiansen J, Løset F, Bhasin RK, Westerdahl H, Vik G. Predicted and measured performance of the 62 m span Norwegian Olympic Ice Hockey Cavern at Gjøvik. International

Journal of Rock Mechanics and Mining Sciences and Geomechanics Abstracts 1994;31(6):617–41.

Barton N. Some new Q-value correlations to assist in site characterization and tunnel design. International Journal of Rock Mechanics and Mining Sciences 2002;39(2):185–216.

Barton N. Rock quality, seismic velocity, attenuation and anisotropy. UK & Netherlands: Taylor & Francis; 2006. 729.

Barton N. Thermal over-closure of joints and rock masses and implications for HLW repositories. In: Proc. of 11th ISRM congress; 2007. p. 109–16.

Barton N. From empiricism, through theory to problem solving in rock engineering. In: Qian QH, Zhou YX, editors. ISRM cong, 6th Müller lecture. Proceedings, Harmonising rock engineering and the environment. Beijing: Taylor & Francis; 2011. p. 3–14.

Barton N, Pandey SK. Numerical modelling of two stoping methods in two Indian mines using degradation of c and mobilization of φ based on Q-parameters. International Journal of Rock Mechanics and Mining Sciences 2011;48(7), 1095–1012.

Hajiabdolmajid V, Martin CD, Kaiser PK. Modelling brittle failure. In: Proc. 4th North American rock mechanics symposium, NARMS 2000. A.A. Balkema; 2000. p. 991–8.

Müller L. The progressive failure in jointed media. In: Proc. of ISRM congress; 1966. p. 679–86 [in German].

Singh B, Raj A, Singh B. Modified Mohr–Coulomb criterion for non-linear triaxial and polyaxial strength of intact rocks. International Journal of Rock Mechanics and Mining Sciences 2011;48(4):546–55.

Singh M, Singh B. Modified Mohr–Coulomb criterion for non-linear triaxial and polyaxial strength of jointed rocks. International Journal of Rock Mechanics and Mining Sciences 2012;51(1):43–52.



Nick Barton has had a long-standing (45 years) interest in how rock joints and artificial fractures behave. These after all, are the remaining components of shear strength of a rock mass, after possible 'intact bridges' have failed at smaller strains. This important reality – the influence of relative amounts of deformation, is ignored in M-C and H-B and GSI equations.

The author's rock-joint related research at Imperial College, with parallel studies by student friends Peter Cundall and John Sharp, started exactly when the first ISRM congress had been held in Lisbon in 1966, where both Patton and Müller stimulated both conscious and sub-conscious contributions, both of which appear in the above article, and will be found with a little searching.

In the case of Patton, stimulation resulted from his simple saw-tooth gypsum-model demonstrations, and the more realistic multiple-scale 'i-values', used to represent the additional shear strength of rough joints. It was the desire to try to produce something more *quantitative*, which set the author on the initial path of creating tension fractures in a weak, brittle, high density model material. Later, 2D 'rock-slope' models with 40,000 blocks were created using the ultimate 'French' double-bladed guillotine method.

During this time the author believes that Cundall started dreaming of smarter ways of creating blocks. Soon μ DEC, then UDEC and finally UDEC-BB became available in the following 15 years. The discovery of the first non-linear shear strength criterion: $\tau = \sigma_n \tan[20 \log_{10}(\sigma_c/\sigma_n + \varphi_b)]$ from shear tests on the above tension fractures proved to be significant a few years later, when '20' and ' σ_c ' and ' φ_b ' (initially = 30°) were replaced (in 1973, and 1977) by the usually *significantly lower*

values of JRC, JCS and φ_r of natural joints. Bandis's scale-effect studies soon followed, and we reached the 'BB' stage of joint coupled-behaviour modelling, which are an integral part of realistic UDEC-BB models, since joints do shear and dilate (and change their apertures and permeability) before peak strength.

When reaching Norway in 1971, the author's interest gradually changed from *rock slope stability* and shear strength of joints, to *tunnel stability* and shear strength of joints and clay-filled discontinuities. During the case-record based, a posteriori (empirical) development of the Q-system in 1973–1974, the remarkable properties of the ratio J_r/J_a were discovered. (See Fig. A.1 for descriptions). The tunnel and cavern case records appeared to have supplied 'friction coefficients'. The angles given by $\tan^{-1}(J_r/J_a)$ were closely resembling $\varphi + i$, φ , and $\varphi - i$, due to dilatant, non-dilatant, and contractile shear of respectively rough joints, planar joints, and clay-filled joints.

Relative block size (RQD/J_n), in addition to inter-block shear strength (J_r/J_a), has proved to be fundamental to the initial assessment of tunnel, cavern (and mine-stope) stability. But boundary conditions J_w and SRF are vitally important – *when boundary conditions are important*, such as in the exceptionally challenging Pinglin and Jinping II tunnels. Of course there are thousands of tunnels with various degrees of challenging conditions. All the above parameters (and boundary conditions) are mobilized each time we create a tunnel, whether we choose to use these rock mass parameters, or to ignore them.

Of particular note is the (unusual) ratio J_n/J_r . When its value is $J_n/J_r \geq 6$, overbreak and almost natural block-caving can occur. (For example: three joint sets are rated as $J_n = 9$. Rough-surfaced but planar joints are rated as $J_r = 1.5$, as in Fig. A.1. So $J_n/J_r = 6$, and over-break is likely to have occurred, increasing the volume of shotcrete, and probably reducing the spacing of rock bolts.) How can we possibly manage without number of joint sets, when classifying rock masses by RMR and GSI?